Journal of Magnetic Resonance 309 (2019) 106599

Contents lists available at ScienceDirect

Journal of Magnetic Resonance

journal homepage: www.elsevier.com/locate/jmr

A multi-purpose, rolled-up, double-helix resonator ☆

Pedro F. Silva, Saraí M. Torres Delgado, Mazin Jouda, Dario Mager, Jan G. Korvink *

Karlsruhe Institute of Technology (KIT), Institute of Microstructure Technology, Karlsruhe 76131, Germany

ARTICLE INFO

Article history:
Received 1 July 2019
Revised 9 September 2019
Accepted 15 September 2019
Available online 18 September 2019

Keywords:
Transverse volume resonator
Adjustable self-resonance
Commercial front-end
Double helix

ABSTRACT

Multilayer flexible substrates offer a means to combine high lateral precision and resolution with roll-up processes, allowing layer-based manufacturing to reach into the third dimension. Here we explore this combination to achieve an otherwise hard-to-manufacture resonator geometry: the double-helix. The use of commercial flexPCB technology enabled optimal winding connections and a versatile adjustment to various operation fields, sample volumes and resonance numbers. The sensitivity of the design is shown to greatly benefit from the fabrication method, though optimal electrical connections and several radially-wound windings, and was measured to outperform an equivalent solenoid despite the known geometrical disadvantage.

1. Introduction

Nuclear magnetic resonance (NMR) is a well-established and powerful technique, with continually expanding fields of application. However, the specifications of each application often require a redesign of the inductive front-end, be it through a change in the frequency of operation, the thermal behaviour of an excitation coil, or the field direction, and requires significant technical expertise and development effort. Simultaneously, whereas in high-field spectrometers the designs are fairly constrained by a need for a large self-resonance frequency (SRF), low-field front-end development is far less constricted and thus more complicated to optimise for each application. An alternative approach would be to leverage a capacitive front-end, through a resonant cavity with a reduced size that relies on the permittivity of the sample, but this only proves viable at higher NMR frequencies, when the wavelength and thus the cavity become acceptably small [1]. Such cavities have a characteristic working frequency, which means that any frequency tuning must be done with a geometrical change or though the addition of dielectric materials/blocks [2].

For these reasons, the authors set out to develop an adjustable low field design, fitting cylindrical samples of various lengths and diameters, targeting a large frequency range, whilst maintaining optimal performance. The resonator itself should have a small incremental volume, for insertion in narrow bores, and a high filling factor and transverse-field geometry, so as to be compatible with both longitudinal and transverse precession fields (B_0). In addition, it would be favourable to have high winding numbers, both radially and axially, a direct interface to the electronics, and a commercial, low-cost fabrication method, as further elaborated on in Section 2.

The previously reported double-helix design is particularly well-suited as a transverse field resonator with high winding numbers, being readily fabricated with flexible printed circuit board (flexPCB) technology. Given that the NMR precession taking place in a plane perpendicular to the B_0 magnetic field of the spectrometer in use, so as to record a change in magnetic flux, the B_1 sensitivity field generated by the measurement coil must also lie therein. This means that resonator development is intrinsically determined by the targeted spectrometer. Even though solenoidal coils are considered the gold-standard for NMR receivers, these are often incompatible with highly homogeneous B_0 fields, which are typically used to generate longitudinal B_0 fields in cylindrical bores. In contrast, permanent-magnet setups, as used in portable NMR, have a transverse magnetic field due to the use of Halbach arrays or gap magnets, allowing for the use of both transverse and longitudinal resonators.

The double-helix design consists of two tilted solenoids, as introduced in the 1970's during the development of transverse superconducting magnets [3], which were then repurposed into NMR as a higher sensitivity radio frequency (RF) transverse resonator [4]. The initial RF design used a single coil with a tilt angle, leaving part of the induction field unused by the NMR receiver, namely the component along the axial B_0 field. A second version [5] used the same tilted coil, with windings connected in parallel, but this time with a secondary coil composed of floating loops with

☆ Fabrication files for the tested structures are given as supplementary material. Information needed for replication can be found in the text.

* Corresponding author.
E-mail address: jan.korvink@kit.edu (J.G. Korvink).

https://doi.org/10.1016/j.jmr.2019.106599
1090-7807/

zero tilt angle. These removed the axial component of the excitation field perpendicular to the loops, through eddy currents, resulting in a transverse resonator. The authors reported an increase in sensitivity of the overall coil, meaning the loops were inductively coupled with the tilted coil and thus redirected the axial component of the signal. A third version with a double-helix and a single winding pair [6] was implemented, analytically approximated, using the approach of Hoult [7], and reported to have a performance above that of a saddle coil, with both designs in their optimised layout. Building upon the state-of-the-art, the present design uses a complete double-helix and explores the benefits of arraying it with an optimal electrical connection, up to the SRF limit.

The coil's implementation results, presented in Section 4, report on the frequency-dependent ideal winding configuration. The direct connection to on-flexPCB electronics, and the ability to adjust winding topology to different experimental conditions, are also shown. In particular, the ability to reconfigure the coil introduces the flexibility to run different experiments, at different frequencies, in different zones of the sample, or even just use a smaller section of the coil to acquire a smaller volume, at a larger sensitivity. Section 5 discusses the relevance of the results obtained, and several follow-up applications are suggested. The fabrication files for the coil are provided in the accompanying materials, and explained in-depth in Section 3.

2. Theory

2.1. Geometrical constraints

Before any design optimisation of a coil can be made, one must first constrain the design to the experiment's limitations, namely the direction of the B_0 magnetic field of the spectrometer in use, as discussed in Section 1. Another consequence of a sub-optimal pairing between a coil geometry and the B_0 field is the introduction of susceptibility mismatches. These originate from the introduction of a para/diamagnetic material close to the sample. Common susceptibilities differ in the ppm range, inducing a geometry-dependent magnetic field inhomogeneity with a similar magnitude. This effect can be mitigated using a long sample so as to have the interface away from the measurable spins, an approach available only for longitudinally-built resonators, or through the use of materials susceptibility-matched to the sample/coil, as used in transversely placed resonators. The latter approach manages to mitigate the problem to the sub-ppm range [8].

Through these considerations, it becomes clear that a transverse resonator is the preferable choice for a better filling factor of cylindrical bores at a low susceptibility mismatch to the sample. However, current transverse designs are limited to saddle, Alderman-Grant, or birdcage designs [9], known to be sub-optimal due to a low sensitivity, a need for high B_0 fields, and a high complexity. Most importantly, these designs are difficult to array with multiple windings placed either along the axial or radial directions, meaning their homogeneity and sensitivity cannot be improved beyond a certain baseline. The double-helix design thus opens up the possibility to create a heavily arrayed resonator with all the benefits of a transverse field.

2.2. Sensitivity and SNR

NMR coils can be implemented in various dimensions and geometries, under varying constraints, but always with the objective of maintaining a high intrinsic sensitivity. A figure of merit defining a coil's performance as an electromagnetic sensor is defined, for a sample volume V_s, as [7]:

$$\mathrm{SNR}_L \propto \int \frac{B_1/i}{\sqrt{\Re(Z_L)}} dV_S \tag{1}$$

where B_1/i is the magnetic field per unit current generated perpendicular to the static B_0 field, and $\Re(Z_L)$ is the AC resistance of the coil. Other dependencies of the SNR are known but are usually hard to improve and well quantified. This optimisation functional is possible due to electromagnetic reciprocity, which inverts the problem of studying the magnetisation precession's induction in the coil, to the simpler analysis of the field generated by the same coil [7].

The sensitivity is then proportional to the signal-to-noise ratio (SNR) entering the first stage of amplification, usually a low noise amplifier (LNA), after which the measurement's SNR is stepwise degraded. This effect is minimised through a high-gain and low-noise LNA which reduces the impact of subsequent stages. Similarly, it is also possible to reduce the LNA's noise contribution by placing the inductor into a resonant circuit with a capacitor. This passive pre-amplification leads to the final SNR given by the adaptation of Friis' equation [9] in voltage terms:

$$\mathrm{SNR}_{out} = \sqrt{\frac{V_{\mathrm{NMR}}^2}{N_{\mathrm{NMR}}^2 + N_{LC}^2 + \left(\frac{N_{\mathrm{LNA}}}{G_Q}\right)^2 + \left(\frac{N_{\mathrm{rest}}}{G_Q G_{\mathrm{LNA}}}\right)^2}} \tag{2}$$

where G_{LNA} is the gain of the LNA, N_i is the noise at each stage, and G_Q is the approximate amplification of the resonating scheme. Noise from the coil and the circuits N_{LC}, which can be mitigated, is shown separately from the intrinsic NMR noise N_{NMR}, for clarity.

This necessary amplification immediately sets a limitation on the design of the resonator, which must enable an impedance transformation to a resistance above 50 Ω. This requires either a matching network to a standard 50 Ω RF system, at which power transfer and the LNA's noise performance are optimal, or a high-impedance amplification with an OPAMP, which also requires an equivalent noise resistance in the hundreds of Ohms.

2.3. Interfacing and arraying

NMR coils are commonly modelled using the simplified approach of a current path at a near DC frequency, with the analytical Biot-Savart law, or more comprehensively through a full-wave FEM solver, sweeping all parameters of the coil. The latter awards few design guidelines when the structure is not computable, which has led to intensive research on analytically solvable designs, namely with a single winding/structure.

Using the former approach, acceptably accurate for low RF frequencies, one can gauge the expected spatial field dependencies with different connections of the basic unit used, depicted in Fig. 1. Consider a multiple winding inductor with perfect coupling between N_r windings, rolled-up radially, as $\Delta R \ll R_0$, which are connected N_p times in parallel, and N_s times in series. Mutual inductive coupling between windings decreases with a factor $1/k$ for increasing incremental distance, and only negligible or scalar AC effects exist (e.g. zero parasitic capacitance and scalar increase of the resistance due to the skin effect). One can trivially write the total resistance of the coil as $R = N_R N_s R_0/N_p$ and its impedance as $L = N_R^2 N_p^{-1}[N_s L_0 + 2M(1 - k^{N_s N_p/2})/(1-k)]$, using the sum of a geometrical series. By conservation of the magnetic energy in an inductor, it is known that $(B_1/i)^2$ is proportional to the inductance, and one can thus state the SNR_L, Q_L and SRF_L as proportional to $\sqrt{L/R}, L/R$ and $L^{-0.5}$ for large $N_s N_p$, respectively (Eq. 3):

$$\mathrm{SNR}_L \propto \sqrt{Q_L} \underset{\sim}{\propto} \sqrt{N_R[L_0 + 2MN_s^{-1}/(1-k)]}\mathrm{SRF}_L \underset{\sim}{\propto} N_R^{-1} \times \sqrt{N_p/[N_s L_0 + 2M/(1-k)]} \tag{3}$$

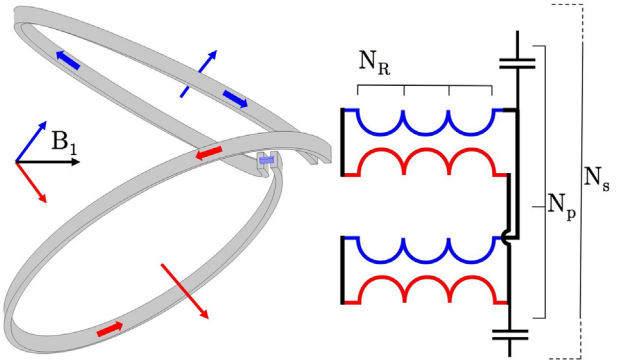

Fig. 1. A single winding of a double-helix coil along with its current directions and correspondent B_1 field is shown on the left. For N_R windings wound radially, the resulting single-helices are connected in series, and then again in series with the other single-helix row. Such a pattern is connected in parallel N_p times and arrayed along the length N_s times. Such a combination may be optionally series-tuned by an on-PCB capacitor, as indicated.

As a first step, the series increase in the coil's resistance is highly favourable, as the introduction of more components/interfaces (e.g. capacitor, switch, solder-joint) is made negligible and the amplified resistance at resonance reaches above the 50 Ω as mentioned above. Beyond this point, it is preferential to generate current in parallel to avoid reducing the overall SRF through an increased parasitic capacitance and a higher inductance. However, this effect is limited in NMR applications due to the proximity effect, as a difference in inductance between parallel windings will shift the current to the edges of the tracks in parallel, drastically reducing excitation/sensing homogeneity. To avoid this, the current must be forced to repeat once again, through a series connection, preferentially achieved by increasing N_r to improve sensitivity.

An inductor can be formed into a resonant circuit, most commonly represented as a parallel LC circuit including the inductance of the coil, based its dominant resistance and using the equivalent capacitance of the matching circuit. This creates a bandwidth reduction, about ω_0, and voltage amplification approximately proportional to Q, defined for an inductor as $\Im(Z)/\Re(Z)$ (Eq. 4):

$$Q_{\mathrm{RLC}} = \frac{\omega_0}{\Delta\omega} = \frac{\omega_0 L}{R} \quad \text{for} \quad \omega_0 = \sqrt{\frac{1}{LC} - \frac{R^2}{L^2}} \tag{4}$$

Introducing only the noise of the capacitive system, which can be made negligible, this technique is used as a low-noise preamplification of the signal by creating a resonant amplification of the NMR signal, as per Eq. (2).

Departing from the lumped component model for the inductor to include a more realistic wave-like behaviour, prevalent at higher frequencies, a spatially varying phase of the current on the metallic conductor and thus also in the generated magnetic field comes to play. This can lead to an inefficient magnetic field or even complete field cancellation, and the length of the coil is then usually limited to $\lambda/10$ for the relevant frequency, as a rule of thumb [10]. This phenomena can nonetheless be re-emerge through the parasitic self-capacitance that a design has among its tracks or with respect to ground, leading to the phenomena of self resonance. As the impedance behaviour of this effect is similar to that of a series tuned RLC system, below the first resonance, one can characterise it as an equivalent capacitance in parallel, despite this having no physical meaning. Even without self-resonance concerns, the introduction of capacitance will result in losses in SNR and Q, due to the introduction of inefficient current paths.

Given the possibility to reduce parasitic capacitances through a narrowing of the tracks, and its inverse effect on the total resistance, one must analyse two effects which will dominate the resistance of a track. These originate from the intra and inter-winding responses to the AC magnetic fields generated, and are respectively known as the skin and proximity effects [11]. The skin effect introduces an increase of the DC resistance of a single standalone track with increasing frequency. For an infinite planar geometry or very high frequencies, one obtains the well known skin depth $\delta = (\pi f \sigma \mu)^{-0.5}$, for wire conductivity σ and permeability μ. This allows one to gauge whether this approximation is valid for the dimensions of the application. Unfortunately, common NMR frequencies entail a copper skin depth in the range of tens to hundreds of micrometers, a magnitude similar to that of the track dimensions used. Simultaneously, the proximity effect cannot be approximated using common strategies due to the similarly sized spacing between tracks. Despite the difficulty in analysis, this regime is known to be the one that most benefits from the arraying techniques presented [12].

Following to the work of Cockroft [13], one can nonetheless obtain some insights into the effects present. The skin effect in a rectangular conductor is well understood and analytically approximable at large frequencies with $R_{AC} = k\sqrt{4fR_{DC}}$, for a geometrical factor k. This dependence functions as a maximiser when compared to the expected linear behaviour at DC. However, due to the distances and frequencies at play, the coupling of both AC effects is far more complex and is reported to have been experimentally verified to be non-monotonous with regards to the inter-winding distance. This means that no further information can be used to optimise track width/spacing. The thickness of the track, t, can nonetheless be freely increased, up to a fabrication limit, to leverage the $\approx t^{-0.5}$ dependence.

3. Resonator design

3.1. Basic-unit geometry

The repeating unit of the resonator, as detailed in [6] and depicted in Fig. 1, consists of two current loops carrying the same forward and return current, patterned with the same tilt angle ϕ. These structures can be arrayed axially one above another, and radially, being rolled around the sample tube N_R times.

This basic unit was parameterised, so as to be implemented on a planar flexPCB of thickness Δ, as shown in Fig. 2, by turning a cylindrical parameterisation of the coil, a function of r, θ and z, to a planar function of x and z only (Eq. 5):

$$\begin{cases} r = (R_0 + \Delta\lfloor\theta/2\pi\rfloor) \\ z = R_0 \tan(\phi)\cos(\theta) \\ 0 \leqslant \theta \leqslant 2\pi N_R \end{cases} \quad \begin{cases} x = \int_0^{2\pi n} \sqrt{r^2 + \left(\frac{dr}{d\theta}\right)^2}\, d\theta \\ = 2\pi R_0 n + \Delta\lfloor n\rfloor\left(n - \frac{\lfloor n\rfloor+1}{2}\right) \\ z = R_0 \tan(\phi)\cos(2\pi n) \\ 0 \leqslant n \leqslant N_R \end{cases} \tag{5}$$

3.2. Arrayed design

The arrayed version of the basic unit in Fig. 1 constitutes a complex problem due to the multi-dimensionality of the unconstrained number of windings, geometrical dimensions, and possible electrical connections. When possible, the dimensions were set using heuristics based on considerations made in Section 2. The design-space was defined by the following dimensions:

- *The cylindrical sample-volume enclosed*: The inner diameter of the sample was defined as the normalising dimension and set to 5 mm, to match standard NMR tubes. The height of the sample, and thus the resonator, will significantly influence perfor-

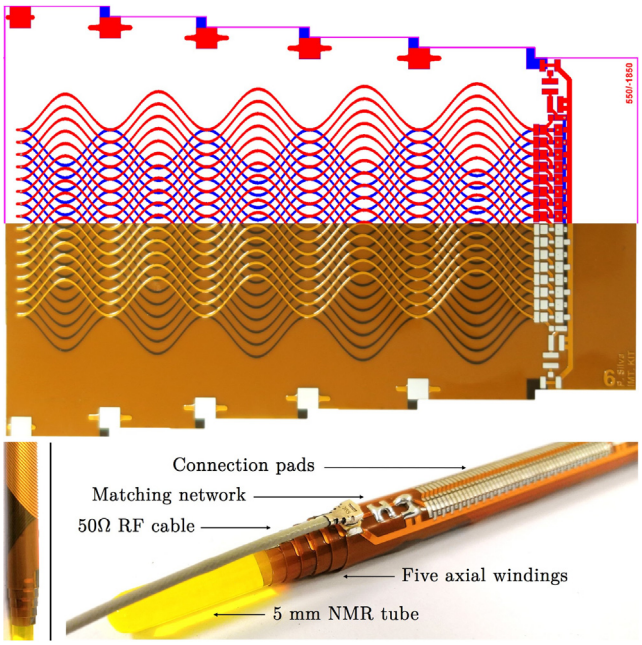

Fig. 2. The schematic (above) and photo (directly below) of the metal traces of a five layer flexible PCB coil design are shown in the top image row. The configuration depicted has 550 μm wide tracks with a 1850 μm gap in-between, along a length of 50 mm. Photographs of the assembled double-helix rolled around a 5 mm NMR sample tube are shown by the two images in the bottom row, where the double helix and the RF connector can be distinguished.

mance and, so as to minimise case-dependent end-effects, the total axial length of the coil was set at 50 mm to have a 1:10 ratio to the diameter. The net result will thus approximate that of an infinite coil with all the windings equally mutually-coupled and a good overall detection homogeneity, known to be critical in several NMR applications [14].

- *The radial distribution of the design*: These dimensions correlate directly to the fabrication stack of the flexPCB, namely the thickness of the copper, dielectric core, and cover layers. The final stack consisted of two 35 μm copper layers, separated by a 50 μm adhesiveless polyimide layer and covered by two 25 μm cover layers, totalling $\Delta \approx 170$ μm. The inner radius of the coil, R_0, was set as 2.55 mm+$\Delta/2$ to match the fabrication guidelines, which require a 10Δ to 20Δ semi-dynamic bending radius. This material stack was then itself stacked as the flexPCB was rolled-up $N_R = 5$ times, a constant across all designs.
- *The axial distribution of the design*: Given that the total patternable planar area is constrained by the sample height and N_R, the copper tracks could be fully characterised by their width, spacing and tilt angle. The tilt angle of the windings to the horizontal was first set to $\phi = 51.43°$, as analytically optimised in [6]. With a custom patterning being straightforward, track width and spacing were left unconstrained and part of the design-space on the fabrication set. Six combinations were thus fabricated above the lower bound of 175 μm arising from the lithography-based fabrication procedure.
- *The electrical connections between windings*: Due to the ability to access both ends of each individual winding, these could be connected in any series and/or parallel combination, or to lumped components, for series-tuning for example. This ability was also left unconstrained, for individual testing, and was enabled by the connection scheme explained and depicted below.

The multi-winding double-helix coils were designed on Altium Designer (Altium Ltd., USA) and manufactured on 2-layer flexPCBs (PCBway, Shenzhen, China). Each flexPCB was rolled around a 5 mm NMR sample tube and constrained by soldering the locking pads above and below the windings so as to maintain structural cohesion and ensure the correct alignment of the various windings. To avoid delamination of the cover layer due to the stress on the pads, they were given elongated structures to better transfer the force to the substrate. Upon receiving the commercially prepared flexPCBs, these were assembled, geometrically constrained, and had the necessary SMD components soldered onto the coil. Assembly was a straightforward process as the locking pads were developed to be soldered sequentially and independently at low temperature, as the top layer pad on winding i only has a thermal connection to the overlapping bottom layer pad on layer $i+1$.

3.3. Adjustment system

The different connection scenarios were possible due to the five type of connection pads on the coil, which are connectable by 0-Ω resistors or simple solder bridges.

In Fig. 3, it becomes clear that the windings and their corresponding pads repeat along the height of the coil, which allows for an arbitrary starting and end point of the active section of the coil. This is possible as all other windings remain electrically floating and disconnected. Likewise, looking at how the windings are connected in parallel, it becomes clear that for the example shown, $N_p = 2$ could be extended to any value, and then put in series N_s times. It is also possible to use the centre pads to connect windings in series with capacitors instead, further improving performance with a series-tuned arrangement.

4. Experimental results

4.1. Sensitivity

To gauge the performance of the proposed coil, according to the insights in Section 2, the Q-factor of the inductor was measured and taken as a proxy for the NMR sensitivity when operating below its self-resonance. As some configurations, namely when most of the windings were connected in parallel, had a low resistance (0.01–1 Ω), these values were taken using a 2-port measurement method [15] with a network analyser (DG8SAQ VNWA 3E, SDR-Kits). The S-parameter measurements were used to derive the Z-parameters and thus R and L. From these values, one could subsequently compute the Q-factor as ωLR^{-1} and the SRF through the resonance condition of $L = 0$, with the results being shown in Fig. 4 for all the configurations tested.

The remaining, unconstrained design-space of the resonator's was the axial density of copper, n_A, a metric for how close together

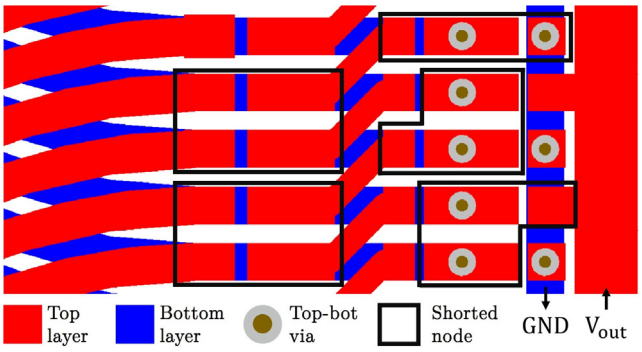

Fig. 3. Schematic of the on-coil connection pads. The shorted node scheme indicated by the black frames using solder connections achieves a coil with $N_s = 2$ and $N_p = 2$.

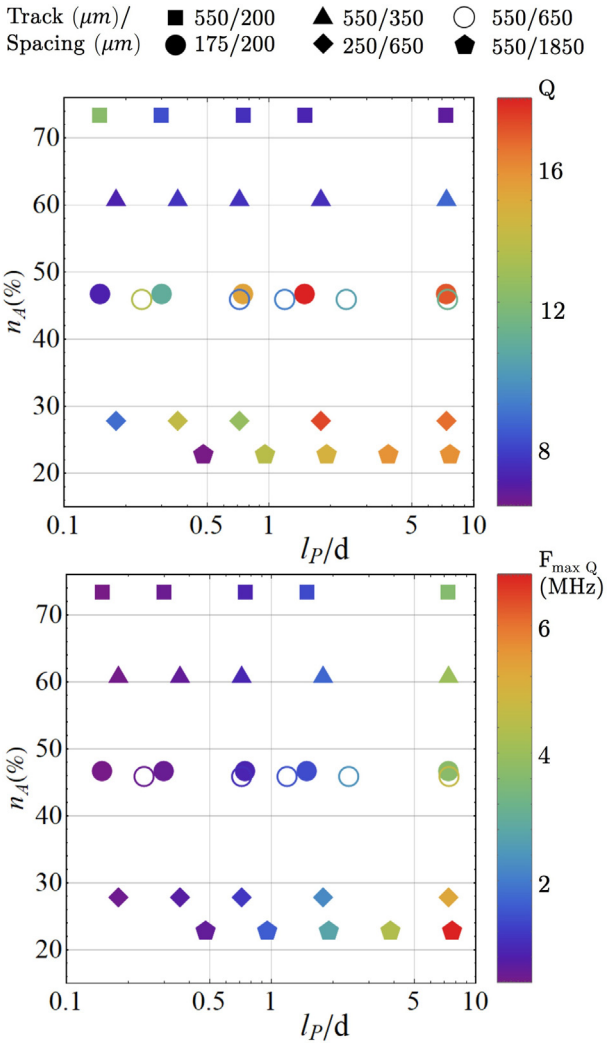

Fig. 4. Frequency-dependent maximum Q for six track configurations and the frequency at which the maximum was found. Results are shown as a function of the axial copper density, n_A, and axial length connected in parallel, l_P, of each configuration.

the windings were patterned compared to their width, and the effective length of current in parallel, l_P, a metric for how the windings were electrically connected together. The latter value, when normalised to the inner diameter of the coil, ranges from a single winding "in parallel", which is then sequentially connected in series to complete the coil, to the full length of the coil connected in parallel, giving l_P/d = 36 mm/5 mm = 7.2.

Interpreting the results obtained, it is clear that the ideal operational frequency increases towards parallel configurations, regardless of n_A, and remains approximately constant when all the windings become fully mutually coupled at moderate n_A values, similarly to the SRF dependency shown in Section 2. The configuration showing the optimal quality factor of 17 at 1.9 MHz was the design with 175/200 μm track/spacing) with a third of its length connected in parallel, sequentially, which landed in the middle of the evaluated design-space. This position indicates a trade-off between increasing the axial copper density, for decreased resistance, and the increasing parasitic capacitance it entails.

A natural follow-up to these results is the comparison of the performance of the double-helix with that of a solenoid, while under a transverse B_0 field. Traditional solenoid implementations suffer from a difficulty in radial arraying, but using the roll-up method shown here, this can be overcome using a stack of planar spirals as the unitary winding. However, the need for a return current for the desired azimuthal current, going radially inwards, makes an high-performance implementation difficult to achieve. Furthermore, a stringent comparison of both designs would require a complete search of the design-space of both geometries and all their frequency-dependent optima, which is clearly not viable. For these reasons, and so as to still allow for a qualitative comparison to the design shown here, two flexPCBs with the same 550/1850 μm width/spacing dimensions were developed. Five radial windings were used in both designs, connected in parallel and put to the test.

To properly compare the performance of both designs, the functional shown in Eq. (1) was computed through the procedure given by Hoult [7]. A 5 mm NMR tube with distilled water and copper sulphate was measured in a commercial 1.05 T system (ICON, Bruker Biospin) using both coils, and their respective input-referred voltages coming from the total water magnetisation of 3.5 mA m^{-1} were obtained. Measuring the impedance profile of the circuits, it was possible to fit them to a lumped model of the circuit and thus obtain the resonant voltage-amplification and resistance at the measuring frequency. These results are shown in Fig. 5 and could be further developed to obtain the sensitivities, found to be 1.9×10^{-6} $TA^{-1}\Omega^{-0.5}$ for the solenoid and 2.9×10^{-6} $TA^{-1}\Omega^{-0.5}$ for the double-helix.

4.2. Configurability

A particular advantage of a design composed of resolderable, floating windings is the ability to tune the electrical behaviour and geometrical profile to better suit, or even enable, a broad array of applications. The configurability showcased here can be leveraged in any other coil geometry, possibly with larger effects.

As an example, given the ability to independently connect different sections of the coil, a dual-resonant matching network was implemented so as to have one section of the coil resonate at one frequency, assigned to ^{1}H, and another section resonant at a different frequency, ^{2}H. Two long capillaries filled with H_2O and D_2O, were measured sequentially at both frequencies, on the two sections of the coil, as shown in Fig. 6. The corresponding nucleus signals are seen to only measurable in their respective coil section, demonstrating that the amplified current resonates only within the desired section, and that the coil can thus be effectively geometrically split.

This approach can simultaneously be implemented with a section-specific electrical connection, so as to perform optimally at different frequencies, due to the ability to independently establish the inter-winding electrical connections. The advantage becomes clear in Fig. 7, where the same track configuration can perform with an optimal quality factor within an approximately 20-fold frequency range, a ratio encompassing the gyromagnetic ratios of all NMR-observable species.

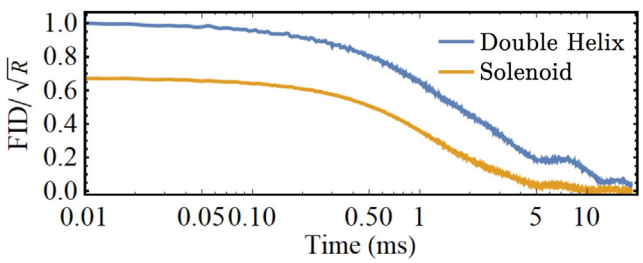

Fig. 5. Envelope of the FID voltages, recorded under identical conditions and at a field of 1.05T, as obtained from equivalent solenoid and double-helix designs after tilt-angle optimisation.

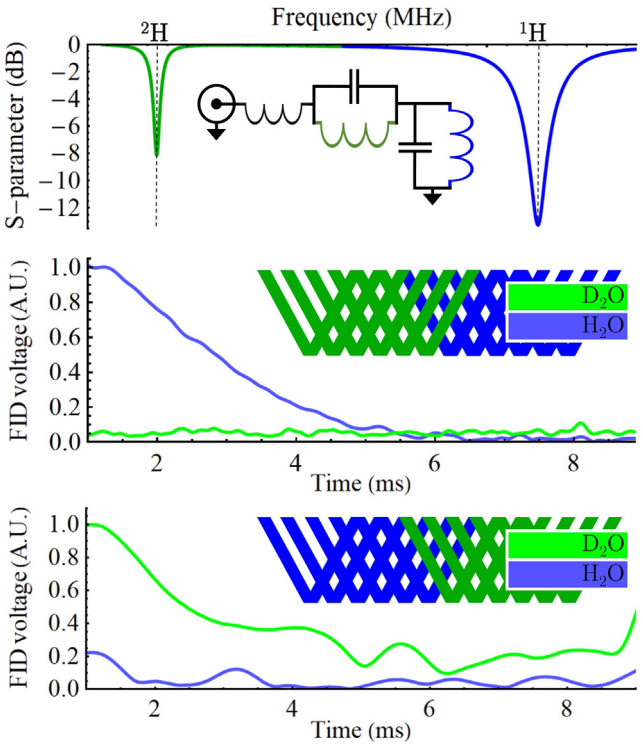

Fig. 6. The S_{11} parameters of the single-port, double-resonant network represented are shown on top, with the resonance corresponding to each section of the coil color-coded in blue (^{1}H) and green (^{2}H). FID envelope measurements of H_2O and D_2O samples in different sections of the coil, using the same pulse sequence, are shown below. (For interpretation of the references to colour in this figure legend, the reader is referred to the web version of this article.)

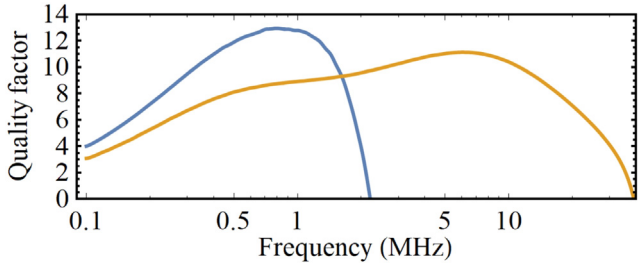

Fig. 7. Frequency dependence of the quality factor for the 550/650 μm geometry connected in series (blue) and in parallel (yellow). (For interpretation of the references to colour in this figure legend, the reader is referred to the web version of this article.)

5. Conclusions

The work shown here demonstrates a successful implementation of a transverse resonator design with a robust, repeatable, and fully commercial fabrication procedure. Despite a severely unconstrained design-space, we aimed to provide some insight into the performance and the possibilities achievable with the design, under the guidance of the appropriate RF theory.

An initial, overarching conclusion arises from the superior performance of the double-helix relative to an equivalent solenoid. Literature establishes that an axially-wound solenoid performs a factor of 3.1 times better than a saddle-coil [7] and a single-winding double-helix performs 10.5% better than an equivalent saddle-coil [6]. Despite the use of a single radial layer and the simplified theoretical treatment, these results qualitatively match the ones measured. Simultaneously, these relationships infer that the fabrication method is incompatible with solenoid-like designs, as their performance is seen to be degraded far below their intrinsic advantage of generating a longitudinal field instead of a transverse one [9]. This suggests that a properly connected double-helix with *multiple radially wound layers* should become the preferred detector for intermediate-frequency applications, where the techniques presented can best be leveraged.

Simultaneously, one could also gauge the effect of *optimal inter-winding electrical connections* on performance. Comparing the blind assumptions for the best implementation, a large axial density of copper fully connected in parallel [5], or an ≈1:3 width-to-spacing design connected in series [6,4], with the best measured design at the optimal frequency, one obtains an improvement of up to 2.7 in the quality factor and consequently of ≈64% in NMR detection sensitivity. This clearly establishes that a track layout must be tested/simulated in varying connection schemes to guarantee an optimal performance in any resonator design.

Beyond direct sensitivity improvements, the proposed design allows an excellent *reconfigurability of the system*. The Q-optimal track implementation, for example, can be reconnected to show an SRF between 1.1 and 30 MHz, which is a sufficient range to measure all NMR-active nuclei in an electrically-adjusted configuration. Beyond this, the ability to geometrically reconfigure the coil means that a single PCB can measure samples of variable size by shortening the coil, can measure multiple resonances by resonating differently in each section, or even include control electronics for more complex behaviour.

The results presented show a *promising future for the technique* as fabrication and application-specific designs improve. With the thickness-to-bending-ratio limitation relaxed, better performing double-helices on flexPCBs will be possible, due to diminishing intra-winding parasitic capacitance, and copper-layer numbers will be increased from the two currently achievable. The latter will prove invaluable when designing decoupled double-helix pairs for longitudinal fields, a promising and easily achieved solution due to the design's patterning precision and ability to turn a planar offset into an angular one, when rolled-up. The axial/radial stacking of several resonators, to be rolled-up together, can be done with different N_r parameters and electrical connections, which allows a large variation in self-resonant frequencies, thus opening the door to integrated EPR/DNP. Fortunately, the magnetic field of a layer/coil-section far above its self-resonance is significantly reduced/shaped, which drastically reduces the mutual coupling to the other inductors rolled together. This can be used to stack multiple near-decoupled groups of resonances, in differing frequency ranges, in different layers/coil-sections, thus avoiding the standard limit of penta-resonant matching networks [16].

Acknowledgements

The authors would like to thank Dr. Neil MacKinnon for helpful and fruitful discussions. PFS acknowledges Bürkert GmbH & Co. KG for funding for this project. ST, DM, and JGK would like to thank the European Union for funding [Grant H2020-FETOPEN-1-2016-2017-737043-TISuMR]. JGK and MJ acknowledge the DFG for partial funding [Contract KO 1883/29-1].

Appendix A. Supplementary material

Supplementary data associated with this article can be found, in the online version, at https://doi.org/10.1016/j.jmr.2019.106599.

References

[1] A.G. Webb, Dielectric materials in magnetic resonance, Concepts Magnetic Reson. Part A 38A (4) (2011) 148–184.

[2] Arnon Neufeld, Naftali Landsberg, Amir Boag, Dielectric inserts for sensitivity and RF magnetic field enhancement in nmr volume coils, J. Magn. Reson. 200 (1) (2009) 49–55.
[3] A.V. Gavrilin, M.D. Bird, S.T. Bole, Y.M. Eyssa, Conceptual design of high transverse field magnets at the NHMFL, IEEE Trans. Appl. Supercond. 12 (1) (2002) 465–469.
[4] Y.H. Sun, G.E. Maciel, The tilted coil for NMR experiments, J. Magnetic Reson., Series A 105 (2) (1993) 145–150.
[5] E. Jeong, D. Kim, M. Kim, S. Lee, J. Suh, Y. Kwon, A solenoid-like coil producing transverse RF fields for MR imaging, J. Magn. Reson. 127 (1997) 73–79.
[6] J. Alonso, A. Soleilhavoup, A. Wong, A. Guiga, D. Sakellariou, Double helix dipole design applied to magnetic resonance: a novel NMR coil, J. Magnetic Reson. 235 (2013) 32–41.
[7] D.I. Hoult, R.E. Richards, The signal-to-noise ratio of the nuclear magnetic resonance experiment, J. Magnetic Reson. (1969) 24 (1) (1976) 71–85.
[8] M.C. Wapler, J. Leupold, I. Dragonu, D. von Elverfeld, M. Zaitsev, U. Wallrabe, Magnetic properties of materials for MR engineering, micro-MR and beyond, J. Magn. Reson. 242 (2014) 233–242.
[9] J. Mispelter, M. Lupu, A. Briguet, NMR Probeheads for Biophysical and Biome: Theoretical Principles and Practical Guidelines, 2nd ed., Imperial College Press, 2006.
[10] J. Thomas Vaughan, Ultra High Field MRI: High-Frequency Coils, Springer, US, 2006, pp. 127–161.
[11] T.L. Peck, R. Magin, P.C. Lauterbur, Design and analysis of microcoils for NMR microscopy, J. Magnetic Reson. Series B 108 (09) (1995) 114–124.
[12] S.C. Grant, L.A. Murphy, R.L. Magin, G. Friedman, Analysis of multilayer radio frequency microcoils for nuclear magnetic resonance spectroscopy, IEEE Trans. Magn. 37 (4) (2001) 2989–2998.
[13] J.D. Cockcroft, Skin effect in rectangular conductors at high frequencies, Proc. Roy. Soc. London A: Math., Phys. Eng. Sci. 122 (790) (1929).
[14] Kevin R. Minard, Robert A. Wind, Solenoidal microcoil design. Part I: Optimizing RF homogeneity and coil dimensions, Concepts Magnetic Reson. 13 (2) (2001) 128–142.
[15] Keysight Technologies. Ultra-low impedance measurements using 2-port measurements. literature.cdn.keysight.com/litweb/pdf/5989-5935EN.pdf. Online application note; accessed 23 May 2019.
[16] H. Davoodi, M. Jouda, J.G. Korvink, N. MacKinnon, V. Badilita, Broadband and multi-resonant sensors for NMR, Prog. Nucl. Magn. Reson. Spectrosc. 112–113 (2019) 34–54.